

STOCHASTIC LATTICE SIMULATIONS OF FLEXURAL FAILURE IN CONCRETE BEAMS

JAN ELIÁŠ*, MIROSLAV VOŘECHOVSKÝ* AND ZDENĚK P. BAŽANT†

*Brno University of Technology, Faculty of Civil Engineering
Veveří 331/95, Brno, 60200, Czech Republic
e-mail: elias.j@fce.vutbr.cz, vorechovsky.m@fce.vutbr.cz

†McCormick School of Engineering and Applied Science, Northwestern University
2145 Sheridan Road, CEE, Evanston, Illinois 60208
e-mail: z-bazant@northwestern.edu

Key words: Lattice-particle model, Spatial randomness, Bending, Fracture energy

Abstract. The contribution employs meso-level discrete numerical model to approximate mechanics of concrete failure. The model represents the material by assembly of rigid-like particles interconnected by nonlinear bonds with strain softening. Spatial material randomness is introduced by varying the local meso-level strengths and fracture energies of inter-particle bonds. The variations are modeled using realizations of stationary autocorrelated random field and studied for two different correlation lengths. The study is focused on maximal load and energy dissipation during the progressive failure. It is found that material fluctuations in *notched* beams do not influence the mean values of maximal load and dissipated energy, but they influence their variance. In the case of *unnotched* beams, the mean of maximal load decreases with decreasing correlation length of material properties; however, the coefficient of variation of the peak load increases.

1 INTRODUCTION

It has been widely recognized that the mechanical properties of materials exhibit spatial variability. The seminal theory of Weibull [27] offered simple and powerful tool to determine the probabilistic distribution of structural strength. However, applicability of the Weibull theory is limited to brittle structures with no stress redistribution prior to the peak load. The Weibull theory lacks any material length scale and the rupture of an infinitely small volume directly causes the failure of the whole structure. The absence of any characteristic length scale also results in spurious infinite strength of infinitely small structures [3, 24]. Moreover, the Weibull theory assumes that the strength at every material point is independent of its sur-

roundings. However, many structures are made of quasibrittle materials such as concrete, ceramics, rock or ice. These structures have the ability to partially redistribute the stresses and thus their failure is triggered by the rupture of some representative volume of a finite size. Also the Weibull assumption of independence stands out against the natural expectation that the local strength fluctuates rather continuously inside the structure.

The advantage of Weibull theory comes from the fact that the mechanics of failure do not interact with the stochastic model—only the elastic stress field is needed. Extension of the Weibull theory for finite internal material length scale requires knowledge of the stress redistribution prior to the peak load. The redistribution can be mimicked by the nonlocal Weibull

theory of Bažant and Xi [8] and Bažant and Novák [5], where probability of failure of material point depends not only on its local stress but also on the stresses in its neighborhood. Therefore, the local stress is replaced by a non-local stress obtained by nonlocal averaging of the (local) elastic stress field [4]. The nonlocal Weibull theory agrees for the large sizes with the local one. For intermediate structural sizes, it predicts higher strengths than the local Weibull theory by virtue of stress redistribution. Unfortunately, in the case of very small structures, the theory is not applicable because the approximation of stress redistribution by nonlocal averaging is too simplistic. Although the nonlocal averaging helps to introduce the material internal length, it is unable to take correctly into account possible spatial correlations of the local material properties.

A laborious option of structural strength estimation is represented by stochastic failure simulations that include proper mechanics of stress redistribution. Such a stochastic analysis can be performed using the finite element method with a sophisticated material constitutive law [26]. The failure of highly heterogeneous materials can also be advantageously estimated via discrete models. These models can be *deterministic*: Bolander and Saito [9], Van Mier and Van Vliet [21] or *stochastic*: Alava et al. [1], Grassl and Bažant [14]. This study adopts the lattice-particle model developed at Northwestern University by G. Cusatis et al. [10, 11] to model the distributed fracturing of concrete. Spatial fluctuations are introduced by modeling the material properties as realizations of a random field.

The following Section 2 briefly describes the deterministic mechanical (lattice-particle) model and Section 3 elucidates how the spatial randomness is incorporated into the model. The model is then used in numerical simulations of failure of notched and unnotched three-point bend beams. The results are presented in Sections 4 (notched beams) and 5 (unnotched beams).

2 DETERMINISTIC MODEL

Modeling of the initiation and propagation of cracks in quasibrittle materials exhibiting strain softening has been studied for several decades. Although this is a difficult task complicated by the distributed damage dissipating energy within a fracture process zone (FPZ) of non-negligible size, realistic results have been achieved by several different approaches; see e.g. Bažant and Planas [7]. The present study is based on the cohesive crack model [2, 7, 16], called sometimes the fictitious crack model. It relies on the assumption that the cohesive stress transmitted across the crack is released gradually as a decreasing function of the crack opening, called the cohesive softening curve. Its main characteristic is the total fracture energy, G_F —a material constant representing the area under the softening cohesive stress-separation curve.

In heterogeneous materials, the dissipation of energy takes place within numerous meso-level cracks inside the FPZ. Direct modeling of such distributed cracking calls for representation of the meso-level structure of material. Models capable of efficiently incorporating the concrete meso-structure should be used. For this purpose, the present analysis will be based on the discrete lattice-particle model developed by Cusatis and Cedolin [12], which is an extension of Cusatis et al. [10, 11].

The material is represented by a discrete three-dimensional assembly of rigid cells. The cells are created by tessellation according to pseudo-random locations and radii of computer generated aggregate pieces or particles. Every cell contains one aggregate (Fig. 1a,b). The cells are interconnected by a set of three nonlinear springs (one normal, n , and two tangential, t_1 , t_2). These are placed at the interfaces between the cells, representing the mineral aggregates in concrete and its surroundings. On the level of rigid cell connection, the cohesive crack model is used to represent cracking in the matrix between the adjacent grains. The interparticle fracturing is assumed to be of damage-mechanics type and is modeled using a single

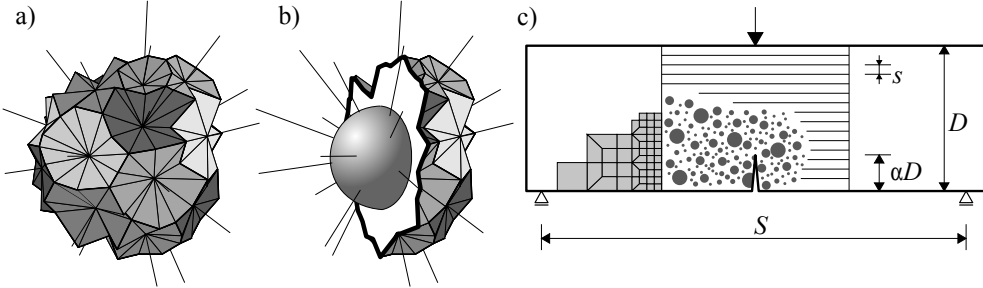


Figure 1: a) One cell of the lattice-particle model and b) its section revealing the aggregate. c) Geometry of the beams simulated in three-point-bending.

damage variable ω applied to all three directions $i = n, t_1$ and t_2 . Forces F_i in the springs can thus be evaluated from their extensions Δu_i by

$$F_i = (1 - \omega)k_i\Delta u_i \quad (1)$$

where k_i is elastic spring stiffness. The damage parameter ω depends on Δu_i and on the previous loading history of each connection. For a detailed description of the connection, the constitutive law and other model features, see Cusatis and Cedolin [12]. The confinement effect (present in the full version of the model) is neglected here because it was estimated to play no important role in the type of experiments studied here.

Beams of depths $D = 300$ mm, span-depth ratio $S/D = 2.4$ and thickness $t = 0.04$ m, were modeled. The maximum aggregate diameter was 9.5 mm. The minimal grain diameter was selected as 3 mm. The aggregate diameters within the chosen range were generated using the Fuller curve. The parameters of the constitutive law of the connection were taken to be similar to those in Cusatis and Cedolin [12], and were as follows: matrix elastic modulus $E_c = 30$ GPa; aggregate elastic modulus $E_a = 90$ GPa; meso-level tensile strength $\sigma_t = 2.7$ MPa; meso-level tensile fracture energy $G_t = 30$ N/m; meso-level shear strength $\sigma_s = 3\sigma_t = 8.1$ MPa; meso-level shear fracture energy $G_s = 480$ N/m; meso-level compressive strength $\sigma_c = 42.3$ MPa; $K_c = 7.8$ GPa; $\alpha = 0.25$; $\beta = 1$; $\mu = 0.2$; $n_c = 2$.

To save computer time, the lattice-particle model covers only the region in which cracking was expected. The surrounding regions of

the beams were assumed to remain linear elastic and were therefore modeled by standard 8-node isoparametric finite elements. The elastic constants for these elements were identified by optimal fitting of a displacement field with homogeneous strain to the displacements of particle system subjected to low-level uniaxial compression. The macroscopic Young's modulus and Poisson ratio were found to equal $\bar{E} = 34.7$ GPa and $\bar{\nu} = 0.19$. The finite element mesh was connected to the system of particles by introducing interface nodes treated as auxiliary zero-diameter particles [13]. These auxiliary particles have their translational degrees of freedom prescribed by shape (or interpolation) functions of the nearest finite element. The rotations of the auxiliary particles were unconstrained.

3 STOCHASTIC MODEL

In the present discrete model, the material properties are assigned at each inter-particle connection according to a stationary autocorrelated random field. The value of the c -th realization of the discretized field at spatial coordinate \mathbf{x} is denoted $\mathbf{H}^c(\mathbf{x})$. For a given coordinate \mathbf{x}_0 , $\mathbf{H}(\mathbf{x}_0)$ is a random variable H of cumulative distribution function (cdf) $F_H(h)$. Since random fields considered are stationary, the cdf $F_H(h)$ is identical for any position \mathbf{x}_0 . The recent studies by Bažant and co-workers [6, 18, 19] showed that, when H represents the strength of a quasibrittle material, $F_H(h)$ can be approximated by a Gaussian distribution onto which a power-law tail is grafted from the left at a probability of about 10^{-4} – 10^{-3} ;

$$F_H(h) = \begin{cases} r_f \left(1 - e^{-\langle h/s_1 \rangle^m}\right) & 0 \leq h \leq h_{\text{gr}} \\ F_H(h_{\text{gr}}) + \frac{r_f}{\delta_G \sqrt{2\pi}} \int_{h_{\text{gr}}}^h e^{-(h-\mu_G)^2/2\delta_G^2} dh & h > h_{\text{gr}} \end{cases} \quad (2a)$$

$$(2b)$$

where $\langle x \rangle = \max(x, 0)$, $s_1 = s_0 r_f^{1/m}$, m is the Weibull modulus (shape parameter) and s_0 is scale parameter of the Weibull tail, μ_G and δ_G are the mean value and the standard deviation of the Gaussian distribution that describes the Gaussian core. The Weibull-Gauss juncture at point at h_{gr} requires that $(dF_H/dh)|_{h_{\text{gr}}^+} = (dF_H/dh)|_{h_{\text{gr}}^-}$; here r_f is a scaling parameter normalizing the distribution to satisfy the condition $F_H(\infty) = 1$. The distribution has 4 independent parameters in total.

The spatial fluctuation of the field is characterized through an autocorrelation function. It determines the spatial dependence pattern between the random variables at any pair of nodes. The correlation coefficient ρ_{ij} between two field variables at coordinates \mathbf{x}_i and \mathbf{x}_j can be assumed to obey the squared exponential function:

$$\rho_{ij} = \exp \left[- \left(\frac{\|\mathbf{x}_i - \mathbf{x}_j\|}{d} \right)^2 \right] \quad (3)$$

It introduces a new parameter d called the auto-correlation length.

To digitally simulate the stationary random field described by the cdf of random variable F_H and the correlation length d in the discrete model, one needs to generate N realizations of the discretized random field $\mathbf{H}^0(\mathbf{x})$, $\mathbf{H}^1(\mathbf{x})$, ..., $\mathbf{H}^{N-1}(\mathbf{x})$ at the facet centers of the model. This is achieved using the Karhunen–Loëve expansion based on the spectral decomposition of covariance matrix \mathbf{C} , where $C_{ij} = \rho_{ij}$. This procedure decomposes the correlated Gaussian variables $\widehat{\mathbf{H}}(\mathbf{x}_i)$ into independent standard Gaussian variables ξ_k , which are easy to generate. The c -th realization of the Gaussian random field $\widehat{\mathbf{H}}^c(\mathbf{x})$ is then obtained using K standard Gaussian ran-

dom variables with the following expression

$$\widehat{\mathbf{H}}^c(\mathbf{x}) = \sum_{k=1}^K \sqrt{\lambda_k} \xi_k^c \psi_k(\mathbf{x}) \quad (4)$$

Here λ and ψ are the eigenvalues and eigenvectors of the covariance matrix \mathbf{C} , and K is the number of eigenmodes or variables considered. In practice, it suffices to employ only a reduced number of eigenmodes $K \ll$ order of \mathbf{C} . In particular, K can be selected such that $\sum_{k=1}^K \lambda_k$ corresponds to about 99% of the trace of the covariance matrix \mathbf{C} [23]. The vectors of independent standard Gaussian variables ξ are generated by Latin Hypercube Sampling using the mean value in each subinterval. The spurious correlation of the variables is then minimized by reordering their K realizations [25].

A non-Gaussian random field can be generated by iso-probabilistic transformation of the underlying Gaussian field, as follows:

$$\mathbf{H}^c(\mathbf{x}) = F_H^{-1}(\Phi(\widehat{\mathbf{H}}^c(\mathbf{x}))) \quad (5)$$

Such a transformation, however, distorts the correlation structure of the field. Thus, when generating Gaussian field $\widehat{\mathbf{H}}$, the correlation coefficients must be modified [23]. This is performed using the approximate method of Hong-Shuang et al. [17].

The realizations of the random field need to be evaluated at every (inter-particle bond) of the mechanical model (at its center). This can be computationally extremely demanding for a large number of facets (with a large covariance matrix) and a short correlation length d (since many eigenvalues are needed so K is large). Therefore, the expansion optimal linear estimation method – EOLE [20], is adopted. This method can significantly reduce the time of random field generation. Instead of the facet centers, the field is initially generated on a regular

grid of nodes with spacing $d/3$ (see Fig. 2). The values of the random field at the facets are then obtain from the expression

$$\widehat{\mathbf{H}}^c(\mathbf{x}) = \sum_{k=1}^K \frac{\xi_k^c}{\sqrt{\lambda_k}} \psi_k^T \mathbf{C}_{xg} \quad (6)$$

where λ and ψ are now the eigenvalues and eigenvectors of the covariance matrix of the grid nodes, and \mathbf{C}_{xg} is a covariance matrix between the facet center at coordinates \mathbf{x} and the grid nodes. After the Gaussian random field values at facet centers are obtained by EOLE (Eq. 6), they need to be transformed to the non-Gaussian space by Eq. 5.

Besides significant time savings, another advantage of using EOLE is that one can simply use the same field realization for several different granular positions. By keeping the c -th realization of decomposed variables ξ^c unchanged, the field realization can be adapted for any configuration of the facets in the discrete model.

The structural strength of a quasibrittle material is typically governed by two important material properties, namely the material strength and the fracture energy. Realistic fracture models should therefore incorporate random spatial variability of at least these two variables. It is reasonable to consider the material strength fully correlated with the fracture energy [14]. Furthermore, the proposed lattice-particle model also includes the shear strength f_s and mode-II fracture energy G_s , which are again assumed to be fully correlated with the tensile strength f_t and mode-I fracture energy G_t , respectively. Assuming identical coefficients of variation (cov), we can use the same realizations of the random field to generate values of material strengths and fracture energies. When any of the four aforementioned mechanical properties are substituted for X , one can write

$$X(\mathbf{x}) = \bar{X} \mathbf{H}(\mathbf{x}) \quad (7)$$

where \bar{X} stands for the mean value of the particular property. The mean value of the (field) random variable H must equal 1.

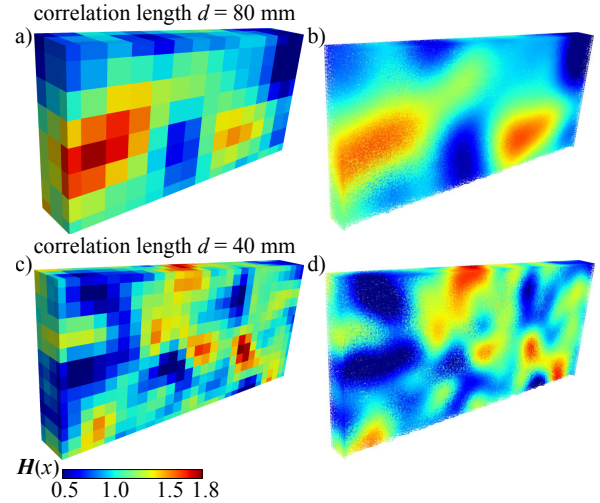


Figure 2: Left: one realization of the autocorrelated random field \mathbf{H} on a grid of spacing $d/3$ for $d = 80$ mm (top) and $d = 40$ mm (bottom). Right: realization of the field \mathbf{H} at the element centers of the lattice-particle model.

In this study, the following parameters of the Weibull-Gauss grafted distribution (Eq. 2a) are used: $m = 24$; $s_1 = 0.486$ MPa; $h_{\text{gr}} = 0.364$ MPa; $\delta_G = 0.25$. These parameters provide the overall mean value $\mu_H = 1$; standard deviation $\delta_H \approx 0.25$, and grafting probability $F_H(h_{\text{gr}}) \approx 10^{-3}$. Two correlation lengths d were considered: a shorter length $d_4 = 40$ mm (according to Grassl and Bažant [14]) and a longer length $d_8 = 80$ mm (according to Vořechovský and Sadílek [26]). The computation is performed with $N = 24$ realizations of the random field for each correlation length.

4 SIMULATIONS OF BENDING OF NOTCHED BEAMS

The beams of the first set (depth $D = 300$ mm, span $S = 2.4D$, thickness $t = 40$ mm) for three-point bending were modeled with a central notch up to 1/6 of beam depth. Ten deterministic simulations were computed. These simulations exhibit a certain scatter because of the pseudo-random granular positions differing for each realization. For both correlation lengths of 40 and 80 mm, 24 simulations with spatial material randomness were performed.

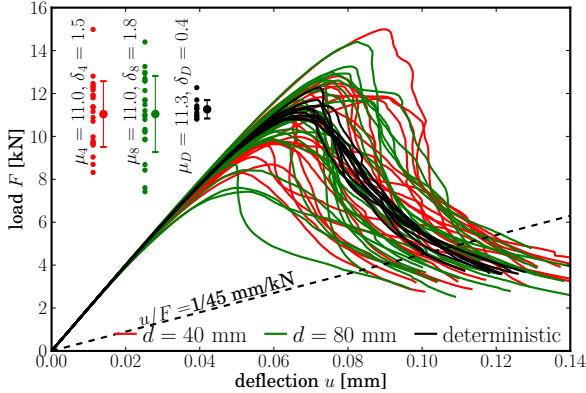


Figure 3: Load-deflection curves for simulations of three-point-bend beams with notch.

All the simulations were terminated when the magnitude of the loading force dropped to 1/3 of the maximum load reached, F_{\max} . To ensure numerical stability in the presence of softening, the simulations were controlled by prescribing an increase of the crack mouth opening displacement (CMOD) in every step.

The notch present in the model induces a stress concentration at the notch tip. Therefore, high stresses occur only in a small area

above the notch tip. Consequently, a crack initiates and propagates always from the notch tip. In stochastic calculations with a rather large correlation length, the local strength fluctuations within the region of high stresses get reduced because of the imposed spatial correlation. Thus, the peak load F_{\max} depends mostly on a single value of the random field realization at the notch tip location. In other words, a random field a with correlation length greater than the length-width ratio of the FPZ can, in the vicinity of the crack tip, be viewed as a randomized constant—the random field becomes a random variable in that region.

The load-deflection curves obtained are shown in Fig. 3. The figure also shows the maximum loads, F_{\max} , in its upper left corner. The effect of the spatial strength fluctuations of the mean value of the maximum load is negligible. The mean value of F_{\max} is, in the deterministic calculation, $\mu_d = 11.3$ kN and, for stochastic simulations with $d = 40$ and 80 mm $\mu_4 = \mu_8 = 11.0$ kN.

However, the standard deviations of the peak

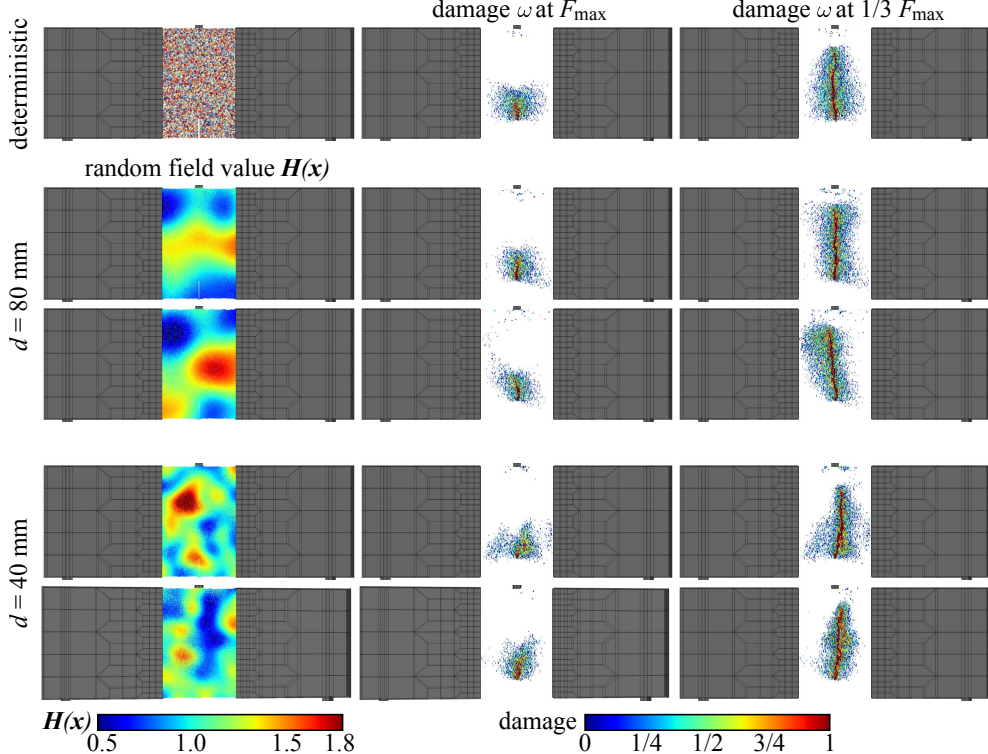


Figure 4: Realizations of random field H (left) and corresponding damage patterns developed in bent notched beams at the peak force (middle) and after the load has dropped to 1/3 of its maximum (right).

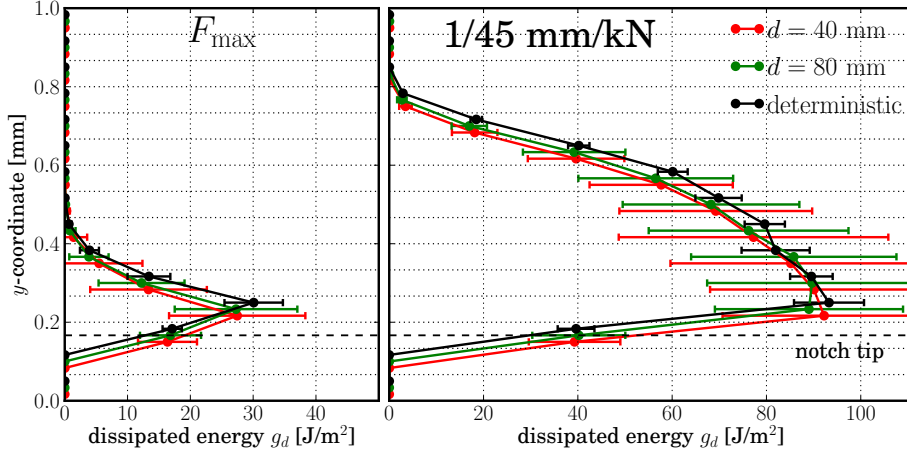


Figure 5: Energy per unit ligament area g_d dissipated in notched beams up to a) the maximum load, and b) reference beam compliance $1/45 \text{ mm/kN}$ as a function of the vertical position in the beam.

load are significantly influenced by the material randomness. The standard deviation of deterministic calculations (given solely by random aggregate position) is $\delta_d = 0.4 \text{ kN}$. A significant increase in the standard deviation is observed for both the correlation lengths $\delta_4 = 1.5 \text{ kN}$ ($d = 40 \text{ mm}$), and $\delta_8 = 1.8 \text{ kN}$ ($d = 80 \text{ mm}$). Since the maximum load of the beam is controlled by the local meso-level strength of a small zone above the notch tip, it is concluded that the fluctuation rate does not influence the standard deviation (unless it is so small that the material parameters vary significantly inside the FPZ).

For several selected realizations, the computed damage patterns (damage parameter ω from Eq. 1) at the peak load and at the termination of the simulations are showed in Fig. 4 together with the corresponding random field realization. Even though one can notice that the crack is slightly attracted (repelled) by areas of low (high) strength, the macrocrack trajectory is similar to the deterministic case (dictated by the singular stress field).

To compare the energy dissipation in the beams, we need to ascertain the simulation stages where the same portion of the ligament has already been damaged. Therefore, we select a stage in which the crack lengths, equivalent according to the LEFM, are equal. Thus, all the models should have at that (reference) stage the same (reference) compliance, chosen

as $1/45 \text{ mm/kN}$ (Fig. 3).

The depth of specimen was divided into horizontal strips of depth s (Fig. 1c). All the energy dissipated at inter-particle contacts within a specific strip was summed into variable G_d . One can normalize that energy by ligament area as $g_d = G_d/st$. The mean values and standard deviations of g_d are plotted in Fig. 5 for every strip at the peak load and at the reference compliance stages. The figure confirms that the mean energy dissipation in notched tests does not change when the spatial material randomness is applied. Similarly to the peak force behavior, standard deviations of dissipated energy increase when randomness is present.

5 SIMULATIONS OF BENDING OF UN-NOTCHED BEAMS

The second simulation set focused on the bending of unnotched beams in which cracks initiate from a smooth bottom surface. Ten deterministic simulations and $N = 24$ simulations with random field for each correlation length were performed. To control the simulation, one needs to find some monotonically increasing variable, and here again the CMOD was used. For unnotched beams with spatially fluctuating meso-level strength, the location of the macrocrack, and thus the position of the crack mouth, is not known in advance. Therefore, several short overlapping intervals were monitored simultaneously and the controlling CMOD was cho-

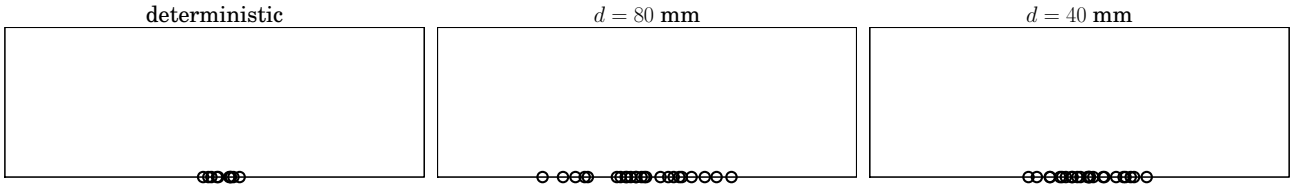


Figure 6: Points of crack initiation of unnotched beams for various degrees of randomness.

sen to be the maximum one among all of them. Note that another possible controlling variable might be the total energy dissipation in the specimen [15].

The variations in the position of the crack mouth of the macrocrack are documented in Fig. 6. The figure demonstrates the fundamental difference between the notched and unnotched situations. When no notch is present, the high-level stress region is much larger, located along the bottom central part of the specimen. The material strength and fracture energy fluctuate within the region and allow the macrocrack to “choose a weak spot” to initiate from. The higher the distance from the midspan, the lower is the tensile stress. In the process of crack(s) formation, the stress field with a certain ability of redistribution increases towards the barrier (or randomly varying strength and energy). The crack would start far from the midspan only when the material strength (and energy) of all points closer to the midspan is significantly higher than in the surrounding region. It is thus expected (and confirmed by Fig. 6) that a short correlation length, resulting in fluctuations that generate the weak spots more frequently, shrinks the zone where the macrocrack initiates. Indeed, the initiation zone for correlation length $d = 80$ mm is wider than it is for $d = 40$ mm.

The load deflection curves obtained from all the simulations performed are plotted in Fig. 7. The upper left corner shows the mean values and standard deviations of the peak load F_{\max} . The greater the fluctuations of the local strength, the weaker is the weakest spot found in the specimen, and thus the lower is the mean value: $\mu_d = 22.4$ kN (deterministic), $\mu_8 = 17.0$ kN ($d = 80$ mm), $\mu_4 = 16.2$ kN

($d = 40$ mm). The standard deviation of the maximum force is low for the deterministic set, where $\delta_d = 0.6$ kN ($\text{cov}_d=2.7\%$). For the correlation length 80 mm, it increases rapidly to $\delta_8 = 3.5$ kN ($\text{cov}_8=21\%$).

When the fluctuation rate increases further ($d = 40$ mm), the standard deviation of F_{\max} drops back to $\delta_4 = 2.1$ kN ($\text{cov}_4=13\%$). This trend arises simply from the fact that the standard deviation of the local strength in the weakest spot inside some fixed region decreases with a decreasing correlation length. Theoretically, the maximum standard deviation of F_{\max} should be obtained for $d \approx \infty$ (which is a situation where the random field can be represented by a random variable—a randomized constant over the specimen volume).

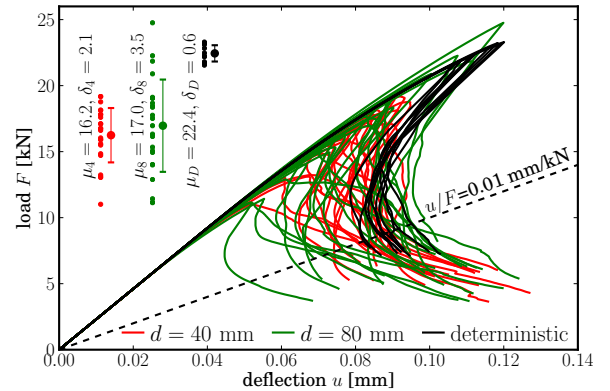


Figure 7: Load-deflection curves for simulations of TPB beams without notch.

Fig. 8 presents several selected realizations of the random field \mathbf{H} and the computed damage patterns. One can see that the damage patterns differ for different levels of randomness. In the deterministic case, the damaged region at the peak load stage spans continuously the entire bottom area and the damage intensity directly depends on the distance from

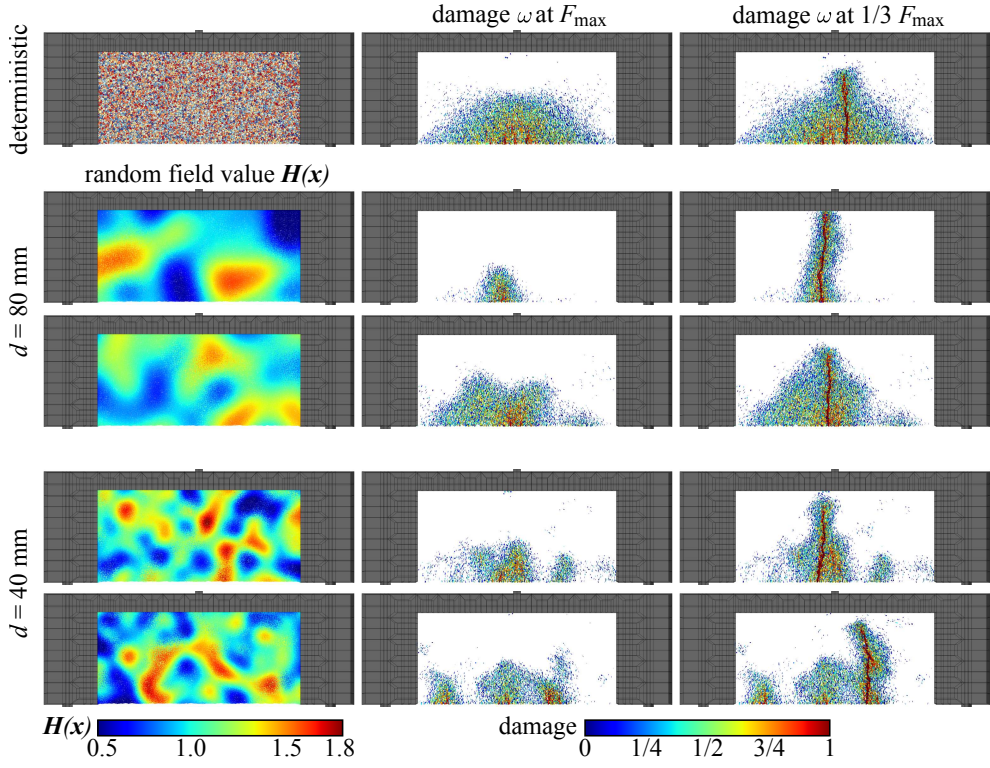


Figure 8: Realizations of random field H (left) and corresponding damage patterns developed in bent beams without notch at the peak force (middle) and after the load dropped to $1/3$ of its maximum (right).

the midspan. For a random local strength and local fracture energy, the damage regions are more localized around low random field values. There is usually one such region for correlation length $d = 40$ mm and several low strength regions for $d = 80$ mm.

To compare the energy dissipation, we again choose some reference compliance that marks stages with the same LEFM crack length. The reference compliance now equals to $1/100$ mm/kN (Fig. 7). Contrary to the results of the notched simulations, the sum of the total energies dissipated in the strips (per unit ligament area) depends on the material randomness. In Fig. 9, the deterministic calculations show higher values of dissipated energy g_d both for the peak force stage and for the stage at the reference compliance.

This is caused by two factors: i) the localized macrocrack propagates in stochastic simulations through areas of lower meso-level strength and meso-level fracture energy, and so less energy is dissipated in total; and ii) distributed pre-peak cracking outside the macrocrack oc-

curs mostly for deterministic simulations and thus it increases the total energy dissipation. Note that from about the middle of the specimen depth upwards, the energy dissipations of deterministic and stochastic simulations match each other again. This is because the crack at that depth cannot choose the weak region as it has already localized, and the stress field forces the crack to grow from the current crack tip, while no pre-peak distributed cracking takes place there.

Finally, let us focus on a deeper analysis of the energy dissipation along the bottom surface. In the bottom boundary strip of width $2d_{\max} = 19$ mm, the dissipated energies (per unit ligament area) inside and outside the macrocrack were evaluated for the peak load stage and for the reference compliance. These values are plotted in Fig. 10, separately for each simulation. The results document that the distributed cracking in the bottommost layer after reaching the peak load is close to zero.

The amount of energy dissipated *outside* the macrocrack is much higher for the deterministic

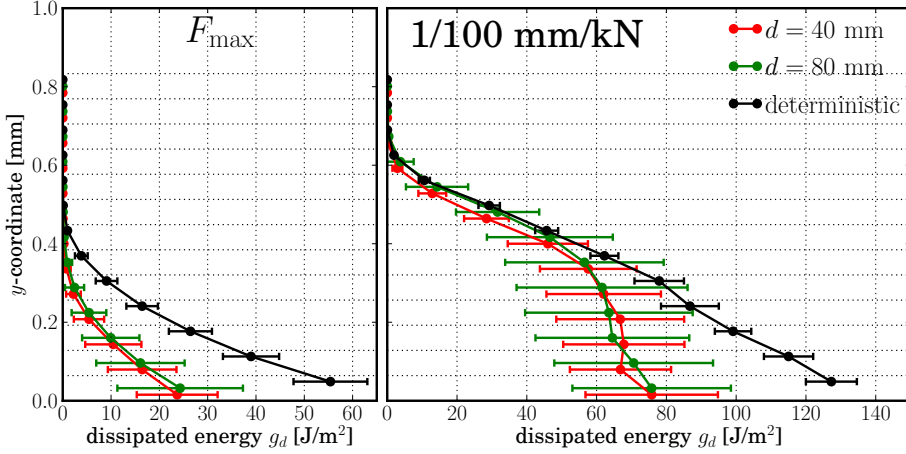


Figure 9: Energy per unit ligament area dissipated in unnotched beams up to a) the maximum load and b) the reference beam compliance $1/100 \text{ mm/kN}$ as a function of the vertical position in the beam.

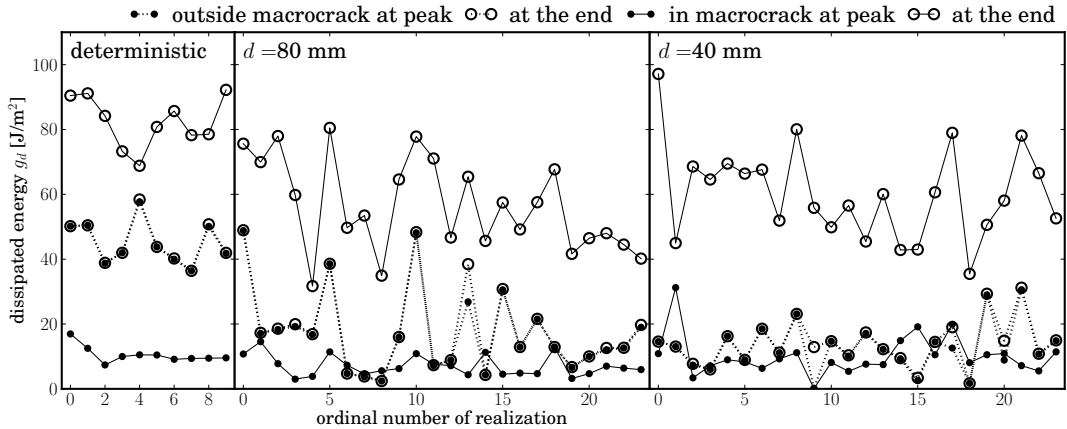


Figure 10: Energy dissipation inside and outside the macrocrack at the peak load and at the reference compliance stages for every simulation.

simulations than for those with random fields. Some of the simulations for $d = 80 \text{ mm}$ reached the value for the deterministic model, which can be explained by the absence of a locally weak spot and subsequent extensive pre-peak distributed cracking (see Fig. 8, third row). The energy dissipated *within* the macrocrack at the reference compliance is clearly higher in the deterministic case than in the stochastic one. This is due to the positive correlation of the local meso-level energy and the meso-level strength at the inter-particle bonds. Since the macrocrack propagates through locally weaker areas, it also dissipates there less energy. The aspects related to the correlation between the local tensile strength and fracture energy have been discussed in [22].

6 SUMMARY AND CONCLUSIONS

The paper analyzes the influence of the spatial randomness of material on the peak load and the energy dissipation, using a discrete lattice-particle model that reflects the meso-scale structure of concrete, particularly the aggregate. The spatial material randomness was introduced by simultaneous scaling of the local meso-level strength and the fracture energy of inter-particle bonds, by means of random realizations of autocorrelated random field. Two basic cases of three-point-bend beams were investigated: i) beams with a notch, and ii) beams without a notch (the modulus of rupture test). The numerical results generally confirm theoretical expectations. The findings are as follows:

(i) In the simulations with a sufficiently deep notch, the crack is forced to start at the notch tip. Therefore, the mean value of the maximum load for notched beam simulations does not change when spatial randomness is present. However, the standard deviation of the maximum load increases when strength randomness is introduced. Also, the energy dissipations in deterministic and random media exhibit the same mean but an increasing standard deviation for the random cases.

(ii) In the case of unnotched beams, the macrocrack initiates in a locally weaker spot. The shorter the correlation length of material properties, the weaker is the statistically weakest initiation spot and thus the lower is the mean maximum load. The standard deviations of the maximum load increase when randomness is introduced. However, shorter correlation lengths lead to a decrease of the standard deviation.

(iii) The energy dissipated in unnotched beams depends on the randomness of the material. Two effects responsible for this dependence are identified: i) A change of the dissipated energy due to correlation of the local meso-level fracture energy and the meso-level strength of inter-particle bonds through which the macrocrack propagates. Depending on the sign of the energy-strength cross-correlation, this effect may increase or decrease the dissipated energy. For the current settings of the model, the lower the local meso-level strength, the lower is the local fracture energy, and the lower is the energy dissipated within the macrocrack. ii) The pre-peak distributed cracking has a tendency to localize in a weaker zone, and thus the material dissipates less energy outside the macrocrack when the random field is introduced.

Acknowledgement

The financial support received from the Czech Science Foundation under Projects Nos. P105/11/P055 and P105/11/1385 (INSREL) is gratefully acknowledged.

References

- [1] Alava, M. J., Nukala, P. K. V. V., and Zapperi, S., 2006. Statistical models of fracture. *Adv. Phys.*, **55**(3-4):349–476.
- [2] Barenblatt, G. I., 1962. Mathematical theory of equilibrium cracks in brittle fracture. *Adv. Appl. Mech.*, **7**:55–129.
- [3] Bažant, Z. P., 2005. *Scaling of Structural Strength*, 2nd updated ed., Elsevier, London.
- [4] Bažant, Z. P., and Jirásek, M., 2002. Non-local integral formulations of plasticity and damage: Survey of progress. *J. Eng. Mech - ASCE*, **128**(11):1119–1149.
- [5] Bažant, Z. P., and Novák, D., 2000. Probabilistic nonlocal theory for quasibrittle fracture initiation and size effect. I. Theory. *J. Eng. Mech - ASCE*, **126**(2):166–174.
- [6] Bažant, Z. P., and Pang, S.-D., 2007. Activation energy based extreme value statistics and size effect in brittle and quasibrittle fracture. *J. Mech. Phys. Solids*, **55**:91–131.
- [7] Bažant, Z. P., and Planas, J., 1998. *Fracture and size effect in concrete and other quasibrittle materials*. CRC Press.
- [8] Bažant, Z. P., and Xi, Y., 1991. Statistical size effect in quasi-brittle structures: II. Nonlocal theory. *J. Eng. Mech - ASCE*, **117**(7):2623–2640.
- [9] Bolander, J. E., and Saito, S., 1998. Fracture analyses using spring networks with random geometry. *Eng. Fract. Mech.*, **61**:569–591.
- [10] Cusatis, G., Bažant, Z., and Cedolin, L., 2003. Confinement-shear lattice model for concrete damage in tension and compression: I. theory. *J. Eng. Mech - ASCE*, **129**:1439–1448.

- [11] Cusatis, G., Bažant, Z., and Cedolin, L., 2006. Confinement-shear lattice csl model for fracture propagation in concrete. *Comput. Method Appl. M.*, **195**:7154–7171.
- [12] Cusatis, G., and Cedolin, L., 2007. Two-scale study of concrete fracturing behaviour. *Eng. Fract. Mech.*, **6**:3–17.
- [13] Eliáš, J., and Bažant, Z., 2011. Fracturing in concrete via lattice-particle model. In Onate, E., and Owen, D., editors, *2nd international conference on particle-based methods - fundamentals and applications*, pages 12, Barcelona, Spain. CD ROM.
- [14] Grassl, P., and Bažant, Z. P., 2009. Random lattice-particle simulation of statistical size effect in quasi-brittle structures failing at crack initiation. *J. Eng. Mech - ASCE*, **135**:85–92.
- [15] Gutiérrez, M. A., 2004. Energy release control for numerical simulations of failure in quasi-brittle solids. *Commun. Numer. Meth. En.*, **20**(1):19–29.
- [16] Hillerborg, A., Modéer, M., and Petersson, P.-E., 1976. Analysis of crack formation and crack growth in concrete by means of fracture mechanics and finite elements. *Cement Concrete Res.*, **6**:773–782.
- [17] HongShuang, L., ZhenZhou, L., and XiuKai, Y., 2008. Nataf transformation based point estimate method. *Chinese Sci. Bull.*, **53**(17):2586–2592.
- [18] Le, J.-L., Bažant, Z.P., and Bazant, M.Z., 2011. Unified nano-mechanics based probabilistic theory of quasibrittle and brittle structures: I. Strength, static crack growth, lifetime and scaling. *J. Mech. Phys. Solids* **59**:1291–1321.
- [19] Le, J.-L. and Bažant, Z.P., 2011. Unified nano-mechanics based probabilistic theory of quasibrittle and brittle structures: II. Fatigue crack growth, lifetime and scaling. *J. Mech. Phys. Solids* **59**: 1322–1337.
- [20] Li, C.-C., and Kiureghian, A. D., 1993. Optimal discretization of random fields. *J. Eng. Mech - ASCE*, **119**(6):1136–1154.
- [21] Van Mier, J. G. M., and Van Vliet, M. R. A., 2003. Influence of microstructure of concrete on size/scale effects in tensile fracture. *Eng. Fract. Mech.*, **70**:2281–2306.
- [22] Vořechovský, M., and Novák, D., 2004. Modeling statistical size effect in concrete by the extreme value theory. In Walraven, J., Blaauwendaad, J., Scarpas, T., and Snijder, B., editors, *5th International Ph.D. Symposium in Civil Engineering, held in Delft, The Netherlands*, Vol. 2, pages 867–875, London, UK. A.A. Balkema Publishers.
- [23] Vořechovský, M., 2008. Simulation of simply cross correlated random fields by series expansion methods. *Struct. Saf.*, **30**:337–363.
- [24] Vořechovský, M., 2010. Incorporation of statistical length scale into Weibull strength theory for composites. *Compos. Struct.*, **92**(9):2027–2034.
- [25] Vořechovský, M., and Novák, D., 2009. Correlation control in small-sample Monte Carlo type simulations I: A simulated annealing approach. *Probabilist. Eng. Mech.*, **24**:452–462.
- [26] Vořechovský, M., and Sadílek, V., 2008. Computational modeling of size effects in concrete specimens under uniaxial tension. *Int. J. Fract.*, **154**:27–49.
- [27] Weibull, W., 1939. The phenomenon of rupture in solids. In *Royal Swedish Institute of Engineering Research*, Vol. 153, pages 1–55, Stockholm.